



Cite this: *RSC Adv.*, 2025, **15**, 25000

Received 3rd June 2025  
 Accepted 4th July 2025

DOI: 10.1039/d5ra03924j  
[rsc.li/rsc-advances](http://rsc.li/rsc-advances)

## Earthworms under threat: assessing the environmental impact of cyhalofop-butyl herbicide on soil health and ecosystem sustainability†

Likun Wang, \* Jiayao Luo, Zixuan Qiu, Mingrong Qian and Kashif Hayat

Cyhalofop-butyl (CyB) is a widely used selective aryloxyphenoxypropionate (AOPPs) herbicide that is primarily applied in paddy fields to control barnyard grass. Despite its extensive use, concerns regarding its ecotoxicological effects on non-target invertebrate organisms, such as earthworm, remain largely unexplored. This study examined the chronic toxicity of CyB on *Eisenia fetida* within the soil. Over a period of 28 days exposure, various biochemical indicators, such as reactive oxygen species (ROS) and associated antioxidant enzymes (SOD, CAT, POD, GST, MDA), were assessed at different exposure concentrations (0–5.0 mg kg<sup>-1</sup>) of CyB. The results demonstrated that CyB exposure could induce significant oxidative stress in earthworms, leading to altered antioxidant enzyme activity and increased lipid peroxidation. Additionally, transcriptomic analysis revealed differential expression genes related to the oxidative stress response and detoxification mechanisms, suggesting potential metabolic disruptions in *Eisenia fetida*. These results would fill the gaps in the toxicity of CyB to earthworm and emphasize the need for further environmental risk assessments to ensure soil ecosystem sustainability.

## 1. Introduction

Pesticides are critical to global agricultural productivity and food security. However, the rapid intensification of agricultural practices over recent decades has led to escalating pesticide use, resulting in widespread environmental contamination.<sup>1</sup> Residues persist in ecosystems, degrading soil and water quality, threatening biodiversity, and posing risks to human health. Among pesticides, herbicides dominate the global market (65%), with disproportionate ecological consequences for soil-dwelling organisms such as earthworms. Following application, approximately 70% of herbicides deposit directly onto soil surfaces, facilitating bioaccumulation and chronic exposure.<sup>2</sup> While regulatory frameworks mandate acute toxicity assessments for non-target species prior to pesticide approval, sublethal effects—particularly on soil organisms and long-term soil health—remain inadequately characterized. Comprehensive evaluation of herbicide-induced sublethal toxicity is, therefore, essential to inform sustainable soil management and ecological risk mitigation.<sup>3</sup>

Cyhalofop-butyl (CyB), butyl (2R)-2-(4-(4-cyano-2-fluorophenoxy)phenoxy)propanoate, a selective aryloxyphenoxypropionate (AOPPs) herbicide, is widely employed for

postemergence control of barnyard grass (*Echinochloa crus-galli*) in rice paddies. Its herbicidal activity arises from its primary metabolite, cyhalofop acid, which inhibits acetyl-CoA carboxylase (ACCase), a key enzyme in fatty acid biosynthesis. By disrupting lipid synthesis, CyB impairs cellular membrane integrity, halts growth, and induces plant mortality.<sup>4,5</sup> However, CyB's environmental persistence and mobility raise concerns: residues detected in Japanese drainage systems (0.01 to 0.08 µg L<sup>-1</sup>)<sup>6</sup> and Chinese rice fields (up to 2.017 mg L<sup>-1</sup>)<sup>7</sup> underscore its potential for bioaccumulation and non-target toxicity.

Emerging evidence highlights CyB's ecotoxicological risks to non-target organisms. Acute exposure induces overt phenotypic effects, including morphological anomalies (e.g., spinal curvature, pericardial edema) in zebrafish embryos at  $\geq 1.00$  mg L<sup>-1</sup>, reduced motility in larvae, and growth inhibition in red swamp crayfish after chronic exposure.<sup>8,9</sup> Sublethal impacts manifest at molecular and histological levels, such as hepatocyte degeneration in zebrafish.<sup>10</sup> Furthermore, CyB exposure leads to a series of morphological changes, including pericardial edema, tail deformation, and spine deformation, in the embryos of *Cyprinus carpio* var.<sup>11</sup> Despite these findings, research on CyB's soil ecotoxicity—particularly to keystone detritivores like earthworms—remains sparse.

Earthworms as ecosystem engineers and bioindicators of soil health, play pivotal roles in nutrient cycling, soil structure maintenance, and contaminant bioremediation. Their dermal sensitivity to xenobiotics, high biomass, and trophic position make them ideal sentinel species for soil ecotoxicology.<sup>12,13</sup> Alterations in earthworm physiology, biochemistry, or

Key Laboratory of Pollution Exposure and Health Intervention of Zhejiang Province, Interdisciplinary Research Academy, Zhejiang Shuren University, Hangzhou 310015, China. E-mail: [wanglikun@zjsru.edu.cn](mailto:wanglikun@zjsru.edu.cn)

† Electronic supplementary information (ESI) available. See DOI: <https://doi.org/10.1039/d5ra03924j>



population dynamics reflect broader ecological disturbances, providing critical thresholds for soil contaminant regulation.<sup>14,15</sup> We hypothesize that earthworm physiological and biochemical responses to soil contaminants can serve as early-warning indicators of ecosystem degradation, enabling the development of predictive models for soil health assessment and contaminant impact evaluation.

This study investigates the chronic ecotoxicity of CyB to earthworms using standardized artificial soil assays. During a 28 day exposure period, oxidative stress indicators were comprehensively assessed every 7 days under sublethal concentrations (0–5.0 mg kg<sup>-1</sup>) of CyB. Besides, complementary transcriptomic analysis elucidated molecular mechanisms underpinning CyB toxicity, leveraging annotated gene expression profiles to identify dysregulated pathways (*e.g.*, regeneration, detoxification). These integrative approaches advance understanding of CyB's sublethal impacts on soil invertebrates, and could offer the critical data for ecological risk assessment of herbicide.

## 2. Materials and methods

### 2.1 Materials

Analytical-grade cyhalofop-butyl (purity  $\geq 96.0\%$ , CAS: 122008-85-9) was offered by Zhejiang Changqing Chemical Co., Ltd (Hangzhou, China). The total protein assay kit, reactive oxygen species assay kit, POD, SOD and CAT assay kits were all purchased from Nanjing Jiancheng Bioengineering Institute. MDA assay kit (TBA method) was from Boxbio Technology Co., Ltd (Beijing, China). All other reagents are analytically pure.

The artificial soil was composed of 10% finely sieved peat moss, 70% quartz sand, and 20% kaolinite. The pH of the soil was adjusted to  $6.0 \pm 0.5$  using calcium carbonate. All the toxicology tests in the present experiment adhered to OECD guidelines.<sup>16</sup>

Earthworms (*Eisenia fetida*) were obtained from a local farm in Hangzhou City, Zhejiang Province, China. They were initially cultured for at least 14 days before the experiment ( $20 \pm 1$  °C). Subsequently, adult earthworms displaying a distinct clitellum and falling within a weight range of approximately 300–600 mg were randomly chosen for use in the formal exposure assay.

### 2.2 Experimental design

CyB at each designated concentration was first thoroughly blended with 100 g of artificial soil to ensure uniform distribution. The mixture was stirred for at least an hour to allow acetone evaporation before being thoroughly blended with 650 g of artificial soil using a household mixer. Distilled water was used to adjust and maintain the final moisture level of the soil at 35%. Subsequently, 750 g of the prepared soil was placed into a 1 L beaker, and 15 earthworms that had been previously acclimated were added. Control samples were prepared similarly, using 5 mL of acetone without CyB. Adequate distilled water and dry cow dung were added weekly to maintain adequate humidity and nutrition for earthworms. Experiments were conducted in a climate chamber (RXZ-500A, Ningbo

Jiangnan Instrument Factory) maintained at a constant temperature of  $20 \pm 1$  °C and a humidity of 75–80%, under a 12 : 12 h light–dark cycle.

### 2.3 Toxicity test and experimental procedures

According to National Standard in China (GB 2763-2021), the maximum residue limit (MRL) of CyB is 0.1 mg kg<sup>-1</sup> for brown rice.<sup>17</sup> The concentrations of CyB in water samples in Japan from block drainage systems range from 0.01–0.08 µg L<sup>-1</sup>.<sup>6</sup> Accordingly, in this subchronic toxicity study, earthworms were subjected to CyB concentrations of 0, 0.1, 0.5, 1.0, 2.5, and 5.0 mg kg<sup>-1</sup> based on the dry weight of artificial soil. On days 7, 14, 21, and 28 following treatment, two earthworms were randomly collected from each beaker—one designated for the measurement of SOD, POD, CAT, GST, and MDA, and the other for ROS analysis. Before conducting assays, the selected earthworms were gently rinsed, weighed, and transferred onto moistened filter paper in Petri dishes. They were kept in the dark at 20 °C for 12 hours to allow for gut clearance.<sup>18</sup> Three replications for each treatment and there are no earthworms died during the whole toxicity test.

### 2.4 Determination of stress biomarkers

**2.4.1 ROS activities.** Following exposure, earthworms were sampled and homogenized to measure ROS and enzyme biomarkers. Reactive oxygen species (ROS) levels were assessed using the 2',7'-dichlorodihydrofluorescein diacetate (DCFH-DA) method, with slight procedural adjustments made to the original protocol.<sup>19</sup> The experimental procedure comprised several key steps. After gut clearance, earthworms from each treatment group were homogenized in pre-chilled potassium phosphate buffer (0.05 mM PBS, pH 7.4) at a ratio of 1 : 10 (w/v). The homogenate was first centrifuged at 3000×g for 12 minutes at 4 °C. The resulting supernatant underwent a second centrifugation at 20 000×g for 16 minutes. Following this, the obtained pellet was resuspended and then incubated with 2 mM DCFH-DA at 37 °C for 30 minutes in a water bath. The reaction was terminated by the addition of hydrochloric acid, and fluorescence intensity was detected using a SpectraMax M2 fluorescence spectrophotometer, with excitation at 488 nm and emission at 522 nm.

**2.4.2 Protein content and enzyme activities.** Earthworms that had cleared their guts were transferred to a glass mortar, ground thoroughly into a fine powder, and then suspended in ice-cold phosphate-buffered saline (PBS, 0.1 mM, pH 7.8) at a ratio of 1 : 10 (w/v), while kept on ice. The resulting homogenate was centrifuged at 3600 rpm for 20 minutes at 4 °C. The supernatant obtained was used to determine total protein levels and measure the activities of SOD, CAT, GST, POD, and MDA. Protein concentration was quantified by the Bradford method,<sup>20</sup> using bovine serum albumin (BSA) as the standard and absorbance measured at 595 nm. The activity of superoxide dismutase (SOD) was assessed following the photochemical reduction method by Giannopolitis and Ries (1977),<sup>21</sup> with one unit (U) of SOD defined as the enzyme quantity required to inhibit 50% of nitroblue tetrazolium (NBT) photoreduction.



Enzyme activities were normalized to protein content and expressed as U per mg protein.

The enzyme activity of CAT was determined according to the method by ref. 22. The activity of the enzyme was determined by monitoring the time-dependent reduction in UV absorbance, which reflects the breakdown of  $\text{H}_2\text{O}_2$  catalyzed by CAT in the sample. One unit (U) of CAT activity corresponds to the amount of enzyme needed to decompose 50% of the  $\text{H}_2\text{O}_2$  within 100 seconds at 25 °C.

The methods introduced previously by ref. 23 were used to determine the POD activity. Initially, guaiacol and hydrogen peroxide ( $\text{H}_2\text{O}_2$ ) were dissolved in phosphate-buffered saline (PBS) to formulate the reaction solution. The reaction mixture was combined with enzyme extract for the sample group and PBS for the control, and changes in UV absorbance at 470 nm were recorded at 30 second intervals over a 3 minute period.

The GST activity was acquired through the method established by ref. 24. The reaction mixture, prepared in a cuvette with a 10 mm light path, included 2.4 mL of phosphate buffer (supplemented with 10% glycerol, 1 mM phenyl-methanesulfonyl fluoride, 1 mM EDTA, and 0.1 mM dithiothreitol, pH 7.5), 0.2 mL of 15 mM reduced glutathione (GSH), 0.2 mL of 15 mM 1-chloro-2,4-dinitrobenzene (CDNB), and 0.2 mL of enzyme-containing supernatant. For the reference cuvette, 2.6 mL of the same phosphate buffer was mixed with 0.2 mL each of 15 mM GSH and CDNB. The absorbance at 340 nm was recorded continuously for 3 minutes to monitor the reaction.

The MDA content was measured *via* a thiobarbituric acid assay which was described by ref. 25. The absorbance of the supernatant was measured at 532 nm, and MDA content was calculated based on the amount of TBA-reactive substances per milligram of protein.

## 2.5 Transcriptome sequencing and analysis

*Eisenia fetida* from the control (CK), 0.1 mg kg<sup>-1</sup> (low concentration), 1.0 mg kg<sup>-1</sup> (medium concentration), and 2.5 mg kg<sup>-1</sup> (high concentration) CyB exposure groups on the day of 21 were used for transcriptomic sequencing. Shanghai Meiji Biotechnology Pharmaceutical Technology Co., Ltd, was commissioned to conduct the whole process. RNA integrity and quality were assessed *via* agarose gel electrophoresis, NanoDrop 2000 spectrophotometry (Thermo Fisher Scientific), and Agilent 5300 Bioanalyzer to ensure OD260/280 between 1.8–2.2 and RQN values greater than 6.5. Only high-quality RNA samples ( $\geq 1 \mu\text{g}$  total RNA, concentration  $\geq 30 \text{ ng } \mu\text{L}^{-1}$ ) were used for downstream applications.

For mRNA library construction, the Illumina® Stranded mRNA Prep, Ligation method was applied. Briefly, polyadenylated mRNA transcripts were isolated by enriching total RNA with magnetic beads conjugated to oligo(dT). The enriched mRNA was fragmented using a specialized buffer and subsequently reverse-transcribed into double-stranded cDNA with random hexamer primers. The cDNA fragments were end-repaired, A-tailed, and ligated to sequencing adapters. Size selection was performed to enrich for fragments around 300–

400 bp. Then the libraries were quantified by using the Qubit 4.0 and sequenced using the NovaSeq X Plus platform (Illumina, PE150).

Initial sequencing reads were processed with fastp to eliminate adapter contamination and low-quality sequences, resulting in high-quality clean reads for downstream analysis. High-quality reads were assembled *de novo* using Trinity, which employs a modular approach (inchworm, chrysalis, and butterfly) to reconstruct transcript sequences without a reference genome. To improve assembly quality, CD-HIT and TransRate were utilized to eliminate duplicate and low-quality sequences. The completeness of the assembly was then assessed with BUSCO by aligning transcripts to a reference set of conserved single-copy orthologs.

Functional annotation of the assembled transcripts was performed by aligning them to various databases—such as NR, Swiss-Prot, Pfam, GO, KEGG, and COG—using Diamond and HMMER tools. Gene Ontology (GO) terms were assigned to transcripts using Blast2GO to categorize. Transcript abundance was estimated using RSEM, and gene expression levels were normalized as TPM (transcripts per million). Differential expression analysis between groups was conducted using DESeq2 (with biological replicates) or DEGseq (without replicates).<sup>26</sup>

To investigate the functional implications of the differentially expressed genes (DEGs), Gene Ontology (GO) and Kyoto Encyclopedia of Genes and Genomes (KEGG) pathway enrichment analyses were carried out using the Goatools toolkit and the scipy module in Python, respectively.<sup>27</sup> Fisher's exact test and Benjamini–Hochberg correction were applied to control the false discovery rate, with a threshold of corrected  $p < 0.05$  for significant enrichment.

## 2.6 Statistical analysis

SPSS 20.0 software were used to analyze the physiological and biochemical indices of earthworms as well as gene expression data. Measurement results were expressed as means  $\pm$  SD. One-way ANOVA followed by Tukey's HSD test was applied for statistical analysis ( $p < 0.05$ ). Differential gene screening was conducted using DESeq2 software, with triplicate samples for each treatment. Figures in the present study were constructed by using the software of Origin (2018).

# 3. Results and discussion

## 3.1 The effect of CyB on the ROS level in earthworms

ROS are generally referred to as oxygen-containing active substances in organisms such as earthworm.<sup>28</sup> Under normal circumstances, their production and elimination maintained in a state of dynamic equilibrium.<sup>29</sup> However, upon exposure to pollutants such as pesticides, organisms may undergo enhanced oxidative reactions, disrupting the dynamic equilibrium and resulting in excessive reactive oxygen species (ROS) accumulation and oxidative damage.<sup>30</sup> Therefore, the ROS level is a sensitive and important indicator reflecting the stress state of an organism.



The changes in the ROS levels of the earthworms when exposed to different CyB were shown in Fig. 1. We can see that the addition of CyB caused only a slight and nonsignificant increase in ROS at  $0.1 \text{ mg kg}^{-1}$ ; however, as the concentration of CyB increased, the ROS level of each treatment group significantly increased on days 7, 14, 21 and 28, indicating that earthworms produced many more ROS under stimulation with CyB than did the control earthworms. As the concentration of CyB in the soil increased, the ROS level also increased, and the results revealed obvious dose-toxicity effects. This result also demonstrated that CyB exposure disturbed the normal dynamic balance between ROS elimination and production, resulting in ROS accumulation in earthworms. As we all known, mitochondria serve as the primary source of reactive oxygen species (ROS) generation and play a central role in mediating oxidative stress signaling pathways,<sup>31</sup> and mitochondrial dysfunction in earthworms can be triggered by oxidative stress arising from an overproduction of ROS.<sup>32</sup> However, after 28 days, the ROS levels in 2.5 and 5.0 mg per kg CyB treatments remained high, indicating that continuous damage to earthworms may further influence the mitochondrial structure and function.

### 3.2 The effects of CyB on enzyme activities in earthworms

Organisms primarily rely on antioxidant enzymes such as superoxide dismutase (SOD), catalase (CAT), and peroxidase (POD) to combat oxidative stress. Among these, SOD is uniquely specialized in removing superoxide anions. In parallel, CAT functions as a vital part of the cellular antioxidant defense system by decomposing hydrogen peroxide ( $\text{H}_2\text{O}_2$ ), thereby preventing its interaction with superoxide ( $\text{O}_2^-$ ) and subsequently limiting the formation of harmful hydroxyl radicals ( $\text{OH}^-$ ), which is essential for maintaining cellular integrity.<sup>33</sup>

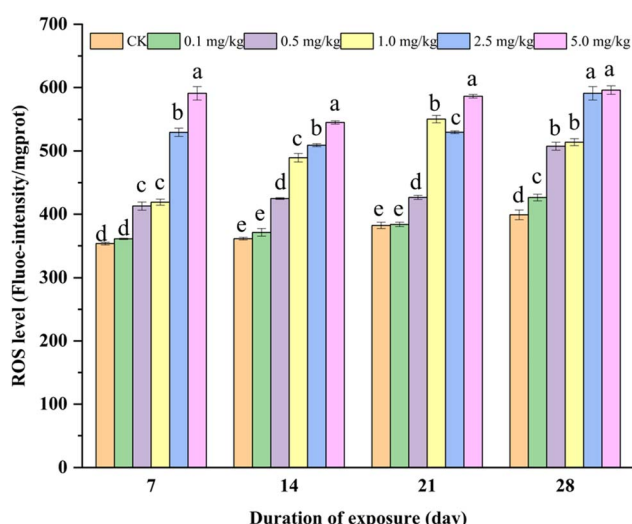
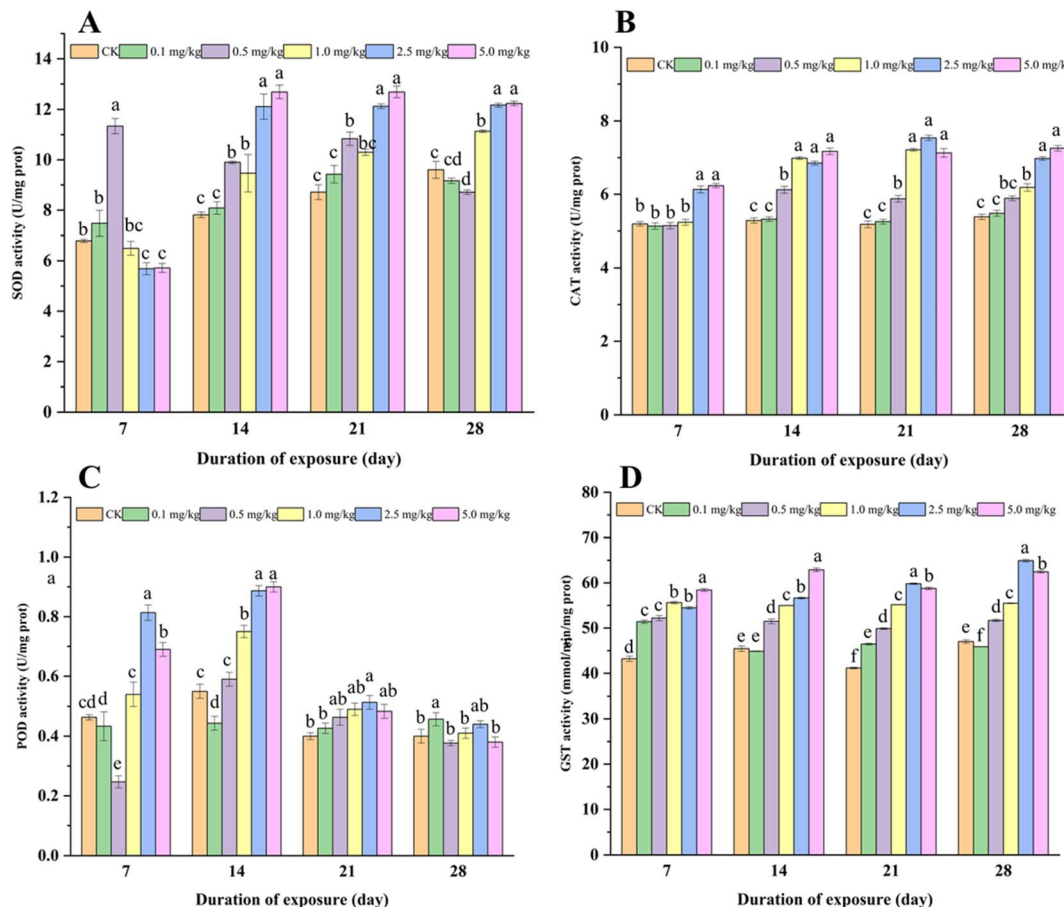


Fig. 1 Effects of different concentrations of CyB on ROS levels in earthworms over a 28 day period exposure. Mean  $\pm$  standard error ( $n = 3$ ) was used to report the data. Different letters above bars indicate significant differences between the treatments of the same day ( $p < 0.05$ ).

As illustrated in Fig. 2(A), the activity of SOD increased after 7 days in all exposure groups except in the  $0.5 \text{ mg kg}^{-1}$  treatment group, which showed a peak at day 7 before declining thereafter. Compared with those in the control group, the SOD in the high-CyB treatment groups ( $1.0$ ,  $2.5$  and  $5.0 \text{ mg kg}^{-1}$ ) tended to increase continuously during the 28 days. The activity of SOD in the low-CyB treatment group ( $0.1 \text{ mg kg}^{-1}$ ) was not significantly different compared with control group during the incubation period ( $p > 0.05$ ). However, the level of SOD in the earthworms with high concentration of CyB significantly increased after treatment during the expose period. These findings suggest that at lower CyB concentrations, SOD activity was not triggered to counteract ROS, whereas higher CyB levels were capable of inducing SOD activation to mitigate excessive reactive oxygen species in earthworms.<sup>34</sup> In the present study, the effects of CyB with moderate ( $0.5 \text{ mg kg}^{-1}$ ) and high concentrations on SOD activity exhibited markedly different patterns. The elevated SOD activity at moderate levels suggests that earthworms may have initiated a defensive response against CyB-induced oxidative stress. In contrast, the observed decline in SOD activity at higher concentrations might be attributed to an excessive accumulation of superoxide anions ( $\text{O}_2^-$ ), surpassing the enzyme's scavenging capacity and consequently leading to its inhibition.<sup>35</sup>

CAT and POD are essential antioxidant enzymes that help eliminate excess free radicals by breaking down the  $\text{H}_2\text{O}_2$  into oxygen and water.<sup>36</sup> Catalase is a widely present enzyme in biological systems, characterized by the presence of a heme moiety at its catalytic site.<sup>37</sup> In many organisms, intracellular hydrogen peroxide is regulated by CAT, which plays a crucial role in preventing cellular injury.<sup>38</sup> In this experiment, Fig. 2(B) indicates that the catalase activity observed in  $0.1 \text{ mg kg}^{-1}$  remained unchanged compared to the untreated group during the experiment, likely due to the inability of such a low CyB concentration to trigger antioxidant enzyme responses. In the treatment group of  $0.5 \text{ mg kg}^{-1}$  and  $1.0 \text{ mg kg}^{-1}$ , the activity of CAT first increased but then decreased over time. However, as the concentration of CyB reached to  $2.5$  and  $5.0$ , the activity of CAT was activated and reached the maximum at 14 d in the  $5.0 \text{ mg kg}^{-1}$  group and at 21 d in the  $2.5 \text{ mg kg}^{-1}$  group. Those findings would suggest that little  $\text{H}_2\text{O}_2$  was induced by low level of CyB stress, while high level of CyB-related stress could produce excess  $\text{H}_2\text{O}_2$  in the cells, which led to the activation of CAT in the earthworm.<sup>28</sup> In this study, as it shown in Fig. 2(C), the activity of POD was significantly increased in the early stages in the high-dose CyB treatment groups. However, after 21 days, the POD activity began to decrease and reached the control level on day 28. Unlike SOD and CAT, which remained high through 28 days, POD peaked early and then declined, indicating a different kinetic response to oxidative stress. This distinct pattern suggests that POD responds rapidly to CyB-induced  $\text{H}_2\text{O}_2$  formation but may later be downregulated or overshadowed by CAT/SOD activity as exposure continues. At 7 and 21 days, no significant difference in POD activity was found between the  $0.1 \text{ mg kg}^{-1}$  group and the control, while a decrease was noted at 14 days, reflecting the inability of a low CyB concentration to stimulate POD response. This outcome may be





**Fig. 2** Antioxidant and detoxification enzyme responses in earthworms subjected to varying CyB concentrations over a 28 day exposure period. Panels display the activity levels of SOD (A), CAT (B), POD (C), and GST (D). Data are shown as mean  $\pm$  standard error (SE), with three biological replicates ( $n = 3$ ). Different letters above bars indicate significant differences between the treatments of the same day ( $p < 0.05$ ).

attributed to the varying responses of earthworms to different CyB doses and the collective influence of multiple antioxidant enzymes.<sup>39</sup>

Extensive research<sup>40</sup> has demonstrated that GST functions as a versatile enzyme, facilitating the conjugation of glutathione with hydrophobic molecules—an essential mechanism for modulating oxidative stress responses at the cellular level. In addition, GST plays a vital role in detoxification processes, contributing to the maintenance of physiological balance in earthworms by reducing oxidative damage induced by reactive free radicals.<sup>41</sup> As it was put in Fig. 2(D), the activities of GSTs treated with different CyB doses were stimulated on the 7th and 14th days. The activities of GSTs exposed to low CyB concentrations (0.1 and 0.5 mg kg<sup>-1</sup>) began to decrease on days 14 and 21, whereas those after treatment with high concentrations (1.0, 2.5 and 5.0 mg kg<sup>-1</sup>) were stimulated in a sustained manner with CyB exposure at 7, 14, 21 and 28 d. GST, a key phase II enzyme in organisms, facilitates the conjugation of glutathione (GSH) with electrophilic compounds, producing water-soluble substances that can be eliminated for detoxification. A high dose of CyB can induce high-level oxidative damage; therefore, more GSTs are activated.<sup>42</sup> At the late stage of exposure in 0.1 mg kg<sup>-1</sup>, the GST activity decreased and was lower than that in the

control group. The observed effect may result from coordinated enzyme interactions that attenuate the influence of external contaminants, thereby reducing the necessity for elevated GST levels.<sup>43</sup>

### 3.3 Effects of CyB on the MDA content in earthworms

As illustrated in Fig. 3, the levels of MDA varied over time among different treatment groups. In the group exposed to 0.1 mg per kg CyB, MDA content showed a temporary rise on day 7, followed by a decline, eventually showing no significant difference from the control by day 28. In contrast, exposure to 1.0 and 2.5 mg kg<sup>-1</sup> led to a notable increase in MDA levels ( $p < 0.05$ ) compared with the control, though a gradual decline was observed by day 28. This reduction may be attributed to the action of antioxidant and detoxifying enzymes that scavenge ROS, along with the organism's ability to repair damaged cells.<sup>44</sup> Notably, in the 5.0 mg kg<sup>-1</sup> group, MDA content stayed elevated throughout the exposure period and only began to decrease at day 28. The increase in the MDA content in the high CyB concentration treatment group indicated the continued occurrence of oxidative damage. Lipid peroxidation is a reaction that occurs in organisms under oxidative stress caused by



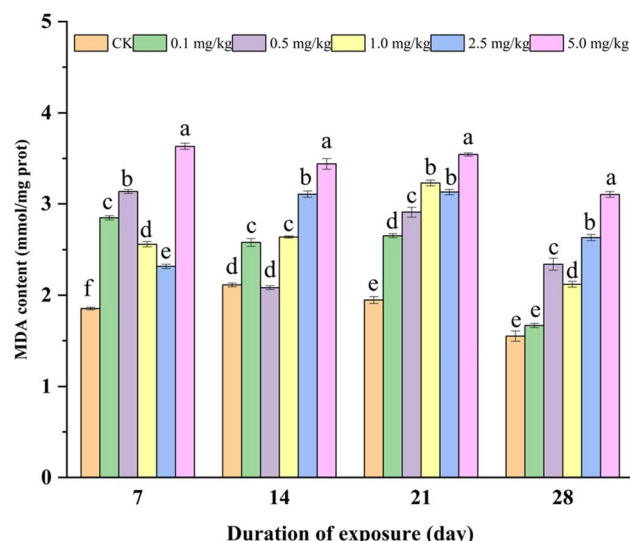


Fig. 3 Changes in MDA levels in earthworms following exposure to various CyB concentrations over a 28 day period. Results are presented as mean  $\pm$  standard error (SE) from three independent replicates ( $n = 3$ ). Different letters above bars indicate significant differences between the treatments of the same day ( $p < 0.05$ ).

pollutants. MDA is an indicator of both lipid peroxidation and the end products of lipid peroxidation, which can lead to severe cytotoxicity.<sup>45</sup> The present study revealed that the MDA content in the high-concentration treatment groups ( $0.5\text{--}5.0\text{ mg kg}^{-1}$ ) was significantly greater than control during 28 days of exposure. The observed effect could be attributed to elevated levels of ROS creating more oxidative imbalance, interfering with intracellular communication, and causing membrane disruption that initiates lipid peroxidation.<sup>46</sup> Therefore, as CyB-treated earthworms generated excess ROS, these ROS likely attacked membrane lipids, resulting in increased MDA levels, concurrently, antioxidant enzymes (SOD, CAT, POD, GST) were upregulated to mitigate the ROS surge, as shown by their elevated activities. This sequence explains the observed lipid peroxidation.

### 3.4 Transcriptomic analysis of the antioxidation and detoxification mechanisms of CyB in earthworms

The mechanisms underlying oxidative stress response and detoxification in earthworms are governed by intricate gene networks. In recent years, transcriptome-based methods have emerged as powerful tools for investigating pollutant-induced shifts in gene expression profiles.<sup>47,48</sup> Fig. 4 presents the preliminary differential expression analysis of earthworm genes following exposure to various CyB concentrations, relative to the control. Comprehensive GO classification and annotation of all identified unigenes are provided in ESI Fig. S1 and S2.<sup>†</sup> The numbers of DEGs detected in the 0.1, 1.0, and 2.5 mg per kg CyB-treated groups were 1246, 1041, and 547, respectively. As shown in the Venn diagram (Fig. 4A), 62 DEGs were commonly expressed across all three treatments, while 957 genes were uniquely regulated in the 0.1 mg  $\text{kg}^{-1}$  group, compared with

736 and 347 exclusive DEGs in the 1.0 mg  $\text{kg}^{-1}$  and 2.5 mg  $\text{kg}^{-1}$  groups, respectively. Relative to the control group, exposure to 0.1 mg per kg CyB resulted in 534 UniGenes being upregulated and 712 downregulated. In the 1.0 mg  $\text{kg}^{-1}$  treatment, 417 genes showed increased expression while 624 were downregulated. Meanwhile, in the 2.5 mg per kg CyB group, a total of 211 upregulated and 336 downregulated UniGenes were identified—fewer than those observed at the lower doses. These findings demonstrate a dose-dependent pattern in transcriptional response: lower CyB concentrations triggered a broader range of gene expression changes, whereas higher concentrations appeared to suppress gene activity more strongly, suggesting a pronounced inhibitory effect at elevated exposure levels.

The KEGG database allows classification of genes based on their associated pathways or functions, enabling the identification of pathways linked to differentially expressed genes (DEGs). KEGG enrichment was applied to assess the functional significance of DEGs, with statistically overrepresented pathways determined *via* hypergeometric distribution tests ( $p < 0.05$ ). Through this approach, DEGs linked to metabolic, signaling, and other vital biological pathways can be pinpointed, highlighting their roles in organismal physiological regulation.<sup>49</sup> The top 20 pathways enriched with the most abundant DEGs exposed to different concentrations of CyB are shown in Fig. 5. Protein digestion and absorption, ECM-receptor interaction, focal adhesion, the PI3K-Akt signaling pathway and human papillomavirus infection were significantly enriched after exposure to different dose of CyB. Meanwhile, different from those in the low- and middle-concentration CyB treatment groups ( $0.1\text{ mg kg}^{-1}$  and  $1.0\text{ mg kg}^{-1}$ ), lipid and atherosclerosis, necroptosis and the IL-17 signalling pathway were significantly enriched in the 2.5 mg per kg CyB treatment group. Details of the upregulated and downregulated KEGG pathways in the different CyB treatment groups compared with those in the control group are shown in Fig. S3.<sup>†</sup>

Protein digestion and absorption (map04974) is essential for acquiring vital nutrients, supporting normal function, and promoting healthy development in animals.<sup>50</sup> It plays a vital role in adapting to nutrient intake fluctuations and is essential for maintaining nutritional homeostasis in animals. Compared with those in the control group, the protein digestion and absorption pathways in all the treatment groups were enriched, which demonstrated that CyB may seriously affect the digestive system of earthworms, which has been widely proven in the context of exposure to other organic pollutants.<sup>51,52</sup> Synthesized by resident cells and exported *via* exocytosis, the ECM forms a spatially organized macromolecular network that provides structural and biochemical support. Cell-ECM interactions occur directly or indirectly *via* surface molecules like integrins, proteoglycans, and CD36, which contribute to intercellular communication, cell adhesion, and the regulation of processes such as cell differentiation.<sup>53</sup> Similar results were also reported in earthworms when they were co-exposed to  $\text{TiO}_2$  nanoparticles and tris(1,3-dichloro-2-propyl) phosphate, whose ECM-receptor interaction was significantly enriched.<sup>54</sup>



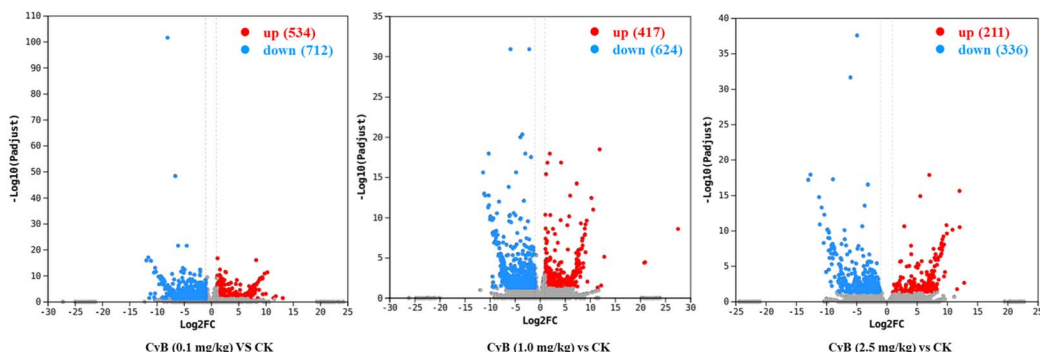


**Fig. 4** Volcano plots illustrate the distribution of differentially expressed genes in the 0.1, 1.0, and 2.5 mg per kg CyB exposure groups relative to the control. The x-axis displays the *p*-value from statistical analysis, while the y-axis denotes the  $\log_2$ -transformed fold change in gene expression. Genes with greater statistical significance appear further along the x-axis. Each point corresponds to an individual gene; red points mark those significantly upregulated, and blue points indicate significant downregulation.

The PI3K–Akt signaling cascade plays a fundamental role in regulating cell proliferation, energy metabolism, and early developmental processes.<sup>55</sup> In the current study, the expression of the gene coding for PI3K was notably enriched in the group treated with CyB. PI3K facilitates the synthesis of phosphatidylinositol-3,4,5-trisphosphate (PIP3) at the plasma membrane, which functions as a secondary messenger that initiates the activation of Akt—a serine/threonine kinase.<sup>56</sup> Once activated, Akt influences various essential cellular pathways, including those governing cell growth, apoptosis inhibition, motility, and the maintenance of gut epithelial integrity. Further oxidative damage and apoptosis are induced in earthworms, thus stressing them and affecting their normal

physiological activities. In conclusion, the immune system, detoxification process and protein metabolism process of earthworm were altered during the remediation process. More biological functions and metabolic pathways in earthworms might be changed with CyB. Certainly, more explicit mechanisms are worthy of further exploration.

Overall, toxic effects on earthworms generally intensified with increasing CyB concentration, higher doses elicited greater ROS accumulation and enzyme perturbation. The transcriptomic data also exhibited a dose pattern, with a broad gene expression response at low/mid doses of CyB and greater gene suppression at the highest dose. These patterns confirm a clear dose–response relationship.

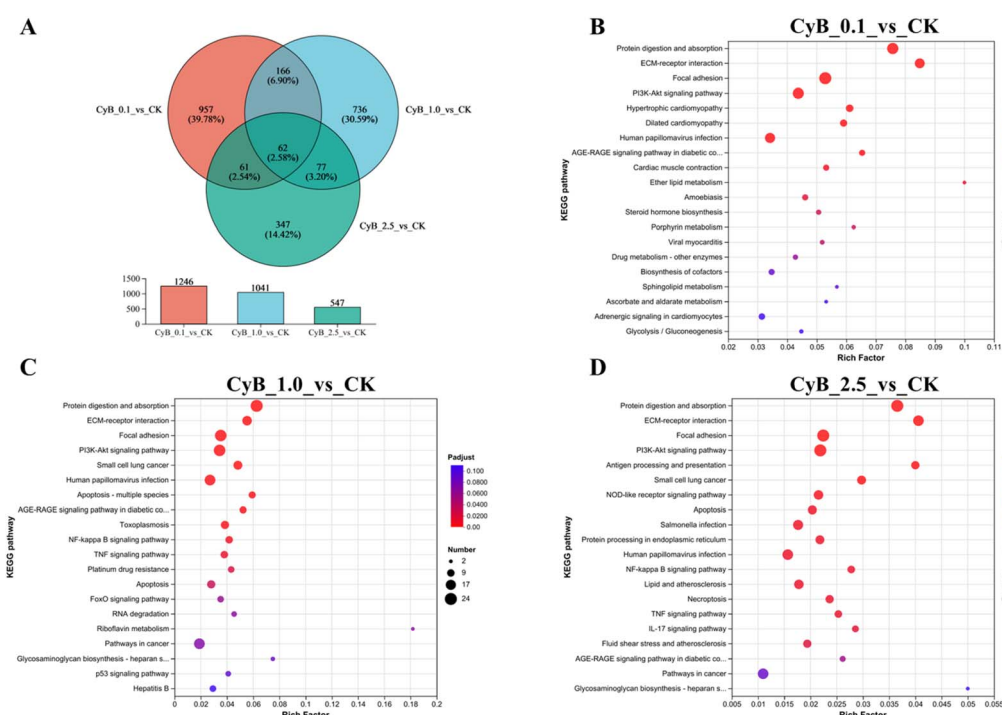


**Fig. 5** Functional characterization of differentially expressed genes (DEGs) in response to 0.1, 1.0, and 2.5 mg per kg CyB exposure was conducted using the KEGG pathway database, with comparisons made against the control group.



In addition, it is important to recognize that the environmental fate of cyhalofop-butyl in natural ecosystems is strongly influenced by external factors such as temperature, soil type, moisture content, and microbial activity. Studies have shown that CyB undergoes rapid degradation in aerobic soil conditions, with its half-life varying significantly depending on environmental parameters.<sup>17,36</sup> For instance, higher temperatures and elevated soil moisture can enhance microbial activity and accelerate herbicide breakdown, whereas cooler or drier conditions may prolong its persistence.<sup>57–59</sup> The current study employed a controlled artificial soil system, which, while valuable for mechanistic insight, does not fully replicate the complexity of field environments. This limitation underscores the need to investigate CyB's ecotoxicological effects under more realistic conditions that account for environmental heterogeneity. Understanding the interaction between environmental factors and pesticide behavior is essential for accurately predicting ecological risks and guiding regulatory decisions. Therefore, future research should focus on field-based assessments and multifactorial experimental designs to better evaluate the long-term and context-dependent impacts of CyB on soil-dwelling organisms and ecosystem health.

## 4. Conclusion

This study provides comprehensive insights into the chronic ecotoxicological effects of CyB on earthworms within a controlled artificial soil–earthworm system. The findings systematically demonstrate that CyB exposure induces pronounced oxidative stress, disrupts antioxidant defense systems (SOD, CAT, POD, and GST), and elevates lipid peroxidation levels in earthworms. These adverse effects exhibit concentration- and duration-dependent amplification, with prolonged exposure resulting in metabolic dysregulation and irreversible cellular damage. The attenuation of enzymatic compensatory mechanisms underscores the organism's limited capacity to mitigate CyB-induced oxidative injury over time.

Transcriptomic profiling further uncovers significant alterations in gene expression networks governing oxidative stress responses, xenobiotic detoxification, and core metabolic processes. Notably, the differential expression of genes (DEGs) involved in protein digestion, ECM–receptor interactions, and apoptosis signaling pathways highlights the systemic physiological disruption caused by CyB. Such molecular perturbations suggest compromised cellular integrity and homeostasis in earthworm, implying broader implications for soil ecosystem functionality.

These results underscore the ecotoxicological risks posed by CyB contamination to soil-dwelling organisms and emphasize its potential to destabilize soil health and ecological balance. Consequently, this study advocates for more stringent regulatory oversight and comprehensive risk assessment frameworks for CyB to mitigate its environmental footprint. Future research should prioritize field-scale validations such as using the local soil rather than the artificial soil, longitudinal analyses of chronic exposure outcomes, and investigations into synergistic interactions with co-occurring agrochemicals. Such efforts are

critical to advancing evidence-based pesticide management practices and safeguarding soil ecosystem resilience.

## Data availability

The datasets generated and/or analyzed during the current study are available from the corresponding author upon reasonable request.

## Author contributions

Likun Wang: writing – original draft, software, investigation, resources. Jiayao Luo: writing – review & editing, software. Zixuan Qiu: software, investigation. Mingrong Qian: writing – review & editing, supervision, conceptualization. Kashif Hayat: writing – review & editing, supervision.

## Conflicts of interest

The authors declare that they have no known competing financial interests or personal relationships that could have appeared to influence the work reported in this paper.

## Acknowledgements

This work was supported by the Zhejiang Provincial Natural Science Foundation of China under Grant No. GN22C140567.

## References

- 1 J. Ma, W. Ren, S. Dai, H. Wang, S. Chen, J. Song, J. Jia, H. Chen, C. Tan, Y. Sui, Y. Teng and Y. Luo, *Sci. Total Environ.*, 2024, **908**, 168439.
- 2 R. J. Yates, E. J. Steel, T. J. Edwards, R. J. Harrison, B. F. Hackney and J. G. Howieson, *Field Crops Res.*, 2024, **308**, 109271.
- 3 T. K. Das, B. Behera, C. P. Nath, S. Ghosh, S. Sen, R. Raj, S. Ghosh, A. R. Sharma, N. T. Yaduraju, A. Nalia, A. Dutta, N. Kumar, R. Singh, H. Pathak, R. G. Singh, K. K. Hazra, P. K. Ghosh, J. Layek, A. Patra and B. Paramanik, *Crop Prot.*, 2024, **181**, 106691.
- 4 Y. Cui, H. Wang, F. Guo, X. Cao, X. Wang, X. Zeng, G. Cui, J. Lin and F. Xu, *Food Chem.*, 2022, **391**, 133241.
- 5 H. Wu, X. Xu, A. Wu, C. Xu, L. Liu, A. Qu and H. Kuang, *Food Biosci.*, 2023, **55**, 102986.
- 6 T. K. Phong, K. Yoshino, K. Hiramatsu, M. Harada and T. Inoue, *Paddy Water Environ.*, 2010, **8**, 361–369.
- 7 Z. Y. Guo, F. Huang and Z. Xu, *J. Ecol. Rural Environ.*, 2008, **24**, 51–54.
- 8 B. Cheng, L. Zou, H. Zhang, Z. Cao, X. Liao, T. Shen, G. Xiong, J. Xiao, H. Liu and H. Lu, *Chemosphere*, 2021, **263**, 127849.
- 9 K. Ou-Yang, T. Feng, Y. Han, J. Li and H. Ma, *Sci. Total Environ.*, 2023, **864**, 161170.
- 10 M. Duan, X. Guo, X. Chen, M. Guo, M. Zhang, H. Xu, C. Wang and Y. Yang, *Aquat. Toxicol.*, 2022, **252**, 106322.



11 X. Xia, P. Wang, R. Wan, W. Huo and Z. Chang, *Environ. Sci. Pollut. Res. Int.*, 2018, **25**, 24305–24315.

12 R. Xiao, A. Ali, Y. Xu, H. Abdelrahman, R. Li, Y. Lin, N. Bolan, S. M. Shaheen, J. Rinklebe and Z. Zhang, *Environ. Int.*, 2022, **158**, 106924.

13 R. Yadav, R. Kumar, R. K. Gupta, T. Kaur, K. Amit, A. Kour, S. Kaur and A. Rajput, *Environ. Adv.*, 2023, **12**, 100374.

14 K. Gudeta, V. Kumar, A. Bhagat, J. M. Julka, S. A. Bhat, F. Ameen, H. Qadri, S. Singh and R. Amarowicz, *Helijon*, 2023, **9**, e14572.

15 F. Wang, Y. Zhang, Y. Su, D. Wu and B. Xie, *J. Environ. Chem. Eng.*, 2024, **12**, 112610.

16 OECD, *OECD Guidelines for the Testing of Chemicals*, 2004, vol. 1.

17 W. Deng, Q. Yang, Y. Chen, M. Yang, Z. Xia, J. Zhu, Y. Chen, J. Cai and S. Yuan, *J. Agric. Food Chem.*, 2020, **68**, 2623–2630.

18 H. Wang, X. Zhang, L. Wang, B. Zhu, W. Guo, W. Liu and J. Wang, *Chemosphere*, 2020, **244**, 125512.

19 J. M. Lawler, W. Song and S. R. Demaree, *Free Radical Biol. Med.*, 2003, **35**, 9–16.

20 M. M. Bradford, *Anal. Biochem.*, 1976, **72**, 248–254.

21 C. N. Giannopolitis and S. K. Ries, *Plant Physiology*, 1977, **59**(2), 309–314.

22 J. B. Xu, X. F. Yuan and P. Z. Lang, *Chin. Environ. Chem.*, 1997, **16**, 73–76.

23 Y. Song, L. S. Zhu, J. Wang, J. H. Wang, W. Liu and H. Xie, *Soil Biol. Biochem.*, 2009, **41**, 905–909.

24 W. H. Habig, M. J. Pabst and W. B. Jakoby, *J. Biol. Chem.*, 1974, **249**, 7130.

25 R. Xiang and D. N. Wang, *Prog. Biochem. Biophys.*, 1990, **17**, 241–242.

26 M. I. Love, W. Huber and S. Anders, *Genome Biol.*, 2014, **15**, 550.

27 G. Yu, L. G. Wang, Y. Han and Q. Y. He, *Omics*, 2012, **16**, 284–287.

28 P. Song, J. Gao, X. Li, C. Zhang, L. Zhu, J. Wang and J. Wang, *Environ. Int.*, 2019, **129**, 10–17.

29 T. Finkel, *J. Cell Biol.*, 2011, **194**, 7–15.

30 M. Valko, D. Leibfritz, J. Moncol, M. T. D. Cronin, M. Mazur and J. Telser, *Int. J. Biochem. Cell Biol.*, 2007, **39**, 44–84.

31 S. Kwon, Y. Lee, Y. Jung, J. H. Kim, B. Baek, B. Lim, J. Lee, I. Kim and J. Lee, *Eur. J. Med. Chem.*, 2018, **148**, 116–127.

32 M. Xu, G. Liu, M. Li, M. Huo, W. Zong and R. Liu, *J. Agric. Food Chem.*, 2019, **68**, 633–641.

33 T. Liu, X. Wang, J. Xu, X. You, D. Chen, F. Wang and Y. Li, *Chemosphere*, 2017, **176**, 156–164.

34 Q. Zhang, M. Saleem and C. Wang, *Sci. Total Environ.*, 2019, **671**, 52–58.

35 T. Liu, X. Wang, X. You, D. Chen, Y. Li and F. Wang, *Ecotoxicol. Environ. Saf.*, 2017, **142**, 489–496.

36 S. Wu, H. Zhang, S. Zhao, J. Wang, H. Li and J. Chen, *Chemosphere*, 2012, **87**, 285–293.

37 C. Glorieux and P. B. Calderon, *Biol. Chem.*, 2017, **398**, 1095–1108.

38 C. Bianchi, A. Y. Kostygov, N. Kraeva, K. Záhonová, E. Horáková, R. Sobotka, J. Lukeš and V. Yurchenko, *Mol. Biochem. Parasitol.*, 2019, **232**, 111199.

39 G. Wang, J. Wang, L. Zhu, J. Wang, H. Li, Y. Zhang, W. Liu and J. Gao, *Arch. Environ. Contam. Toxicol.*, 2018, **74**, 527–538.

40 C. Tang, H. Zhou, Y. Zhu, J. Huang and G. Wang, *Acta Trop.*, 2019, **191**, 8–12.

41 S. Yin, G. Li, M. Liu, C. Wen and Y. Zhao, *Environ. Sci. Pollut. Res.*, 2018, **25**, 18570–18578.

42 J. D. Hayes, J. U. Flanagan and I. R. Jowsey, *Annu. Rev. Pharmacol. Toxicol.*, 2005, **45**, 51–88.

43 T. Ma, W. Zhou, L. K. Chen, L. Wu, P. Christie, H. Zhang and Y. Luo, *PLoS One*, 2017, **12**, e173957.

44 S. Wen, C. Liu, Y. Wang, Y. Xue, X. Wang, J. Wang, X. Xia and Y. M. Kim, *Chemosphere*, 2021, **264**, 128499.

45 Q. Zhang, L. Zhu, J. Wang, H. Xie, J. Wang, Y. Han and J. Yang, *Environ. Sci. Pollut. Res.*, 2013, **20**, 201–208.

46 B. Halliwell and S. Chirico, *Am. J. Clin. Nutr.*, 1993, **57**, 715S–725S.

47 T. Liu, Y. Liu, K. Fang, X. Zhang and X. Wang, *Environ. Pollut.*, 2020, **265**, 115100.

48 M. Mkhinini, I. Boughattas, N. Bousserhine and M. Banni, *Environ. Sci. Pollut. Res.*, 2019, **26**, 2851–2863.

49 L. Chai, Y. Yang, H. Yang, Y. Zhao and H. Wang, *Chemosphere*, 2020, **240**, 124902.

50 X. Gao, J. Chen, K. Yu, Y. Bu, L. Wang and X. Yu, *Mar. Pollut. Bull.*, 2025, **210**, 117331.

51 X. Jiang, Y. Chang, T. Zhang, Y. Qiao, G. Klobučar and M. Li, *Environ. Pollut.*, 2020, **259**, 113896.

52 Z. Qiao, X. Yao, X. Liu, J. Zhang, Q. Du, F. Zhang, X. Li and X. Jiang, *Ecotoxicol. Environ. Saf.*, 2021, **209**, 111824.

53 C. Bonnans, J. Chou and Z. Werb, *Nat. Rev. Mol. Cell Biol.*, 2014, **15**, 786–801.

54 Y. Zhu, X. Wu, Y. Liu, J. Zhang and D. Lin, *Ecotoxicol. Environ. Saf.*, 2021, **208**, 111462.

55 Y. Liu, M. Chen, X. Mu, X. Wang, M. Zhang, Y. Yin and K. Wang, *Environ. Pollut.*, 2023, **327**, 121584.

56 L. Reilly, E. R. Semenza, G. Koshkaryan, S. Mishra, S. Chatterjee, E. Abramson, P. Mishra, Y. Sei, S. A. Wank, M. Donowitz, S. H. Snyder and P. Guha, *Iscience*, 2023, **26**, 106623.

57 C. Zuo, X. Tai, Z. Jiang, M. Liu, J. Jiang, Q. Su and X. Yan, *Molecules*, 2023, **28**, 3495.

58 X. Pan, F. Kong and M. Xing, *Res. Chem. Intermed.*, 2022, **48**, 2837–2855.

59 K. Li, X. Yang, T. Zhao, J. Liu, J. Liu, Y. Li, F. Li, X. Tai and S. Cao, *ChemistrySelect*, 2019, **4**, 10506–10509.

